Ecofriendly Wood Adhesives from Date Palm Fronds Lignin for Plywood

Hiba Ibrahim Huzyan, Alia Abdul Aziz, and M. Hazwan Hussin *

Utilization of lignin phenol glyoxal (LPG) resins was studied as a potential alternative for phenol formaldehyde (PF) resins. Lignin was extracted by alkaline pulping processes (kraft and soda) from date palm fronds (DPF) and was used as an alternative for phenol in LPG resins. The isolated lignin samples were characterized using complementary analyses that included Fourier transform infrared (FTIR) spectroscopy, ^{13}C nuclear magnetic resonance (NMR) spectroscopy, thermal stability, thermogravimetric analysis (TGA), and differential scanning calorimetry (DSC). Kraft lignin phenol glyoxal (KLPG) and soda lignin phenol glyoxal (SLPG) resins also were characterized in terms of solid content, viscosity, and gel time. Finally, physico-mechanical tests were performed on plywood panels that were treated with different molar ratios of LPG resins. The results revealed that 50% (w/w) KLPG resin resulted in higher tensile strength (65.3 MPa) than PF resin (58.57 MPa), which was potentially attributed to the higher amount of phenolic groups compared to soda lignin. Therefore, the substitution of DPF lignin in LPG resins enhanced the adhesive in terms of its chemical and mechanical properties, enabling it to produce a more environmentally friendly wood adhesive.

Keywords: Lignin; Wood adhesive; Date palm fronds

Contact information: Materials Technology Research Group (MaTReC), School of Chemical Sciences, Universiti Sains Malaysia, 11800 Minden, Penang, Malaysia;
** Corresponding author: mhh@usm.my; mhh.usm@gmail.com*

INTRODUCTION

Phenolic resins are credited as the oldest synthetic thermosetting polymers. Due to their outstanding chemical and mechanical properties and characteristics, *i.e.*, high water resistance, dimensional and thermal stability, chemical resistance, and electrical insulation, they are widely applied as acid-resistant coatings, fiber-reinforced composites, electric laminates, and in wood industrial production of exterior-grade plywood panels, oriented strand board panels, and particleboards (Danielson and Simonson 1998; Ramires *et al*. 2010; Foyer *et al.* 2016b). However, the toxicity of formaldehyde (McGregor *et al*. 2006) and the potential shortage of phenol production from the non-renewable petrochemical resources have triggered researchers to conduct numerous studies to investigate possible alternative ecofriendly substances as a replacement to petroleum-based materials in phenol formaldehyde resins (Wu 1997; Ibrahim *et al*. 2011). Some of the bio-based polymers that have been used are proteins, tannins, lignin, and polysaccharides (Ballerini *et al.* 2005; Moubarik *et al.* 2015; Hussin *et al*. 2017).

Lignin is known as a complex phenolic polymer that is built up by oxidative coupling of three major phenylpropanoid units, namely trans-*para*-coumaryl alcohol, trans-coniferyl alcohol, and trans-sinapyl alcohol. Thus, it is characterized by having a high aromatic density and high cross-linked structure that is comparable to phenol network

structure (Ibrahim *et al*. 2007). The functional groups in unmodified lignin are mainly aliphatic and aromatic hydroxyl groups, and methoxyl groups, of which the phenolic –OH groups play a main role in substitution reactions. The structure similarity between phenol and lignin renders the condensation reaction between phenol and formaldehyde in phenolic resins the same as the condensation reaction between lignin and glyoxal in lignin phenol glyoxal resins (Younesi-Kordkheili and Pizzi 2019). Currently, lignin has been isolated from different lignocellulosic waste and exploited in phenol-formaldehyde adhesives as a phenol substituent, due to the structural similarity of both polymers (Zhang *et al.* 2013).

One of the types of lignocellulosic biomass that lignin could be isolated from is date palm fronds. Date palm trees (*Phoenix dactylifera*) are widely cultivated across Northern Africa and the Middle East and are naturalized in many tropical and subtropical regions worldwide. Analysis of date palm trees showed a low to medium hemicelluloses content (13% to 31%), cellulose (33% to 48%), a high ash content (1% to 15%), and extractives (8% to 33%) comparing to other lignocellulosic materials, and a moderate lignin amount (26% to 40%). More specifically, date palm fronds presented 26% of lignin, which is similar to those found in other wood species and non-wood plants (Nasser *et al*. 2016). The reasonable lignin content in the fronds, the increasing amount of waste from the date palm trees that can reach 40 kg (most of them are leaves and surface fibers around the trunk) in a country like UAE (Mallaki and Fatehi 2014), were the reason behind choosing the date palm fronds as a lignin source.

Furthermore, formaldehyde is regarded as carcinogenic by the International Agency for Research on Cancer (IARC) and the Scientific Committee on Occupational Exposure Limits (SCOEL) (IARC 2006). Thus, to produce an environmentally friendly wood adhesive, formaldehyde can be fully replaced by hexamine, glyoxal, and furanic materials (*i.e.*, furfural and furfuryl alcohol) (Norström *et al.* 2014; Foyer *et al*. 2016a; Santiago-Medina *et al*. 2016; Hussin *et al.* 2019). Glyoxal is considered as a non-toxic aldehyde, which is non-volatile, biodegradable, and has a low cost. In addition, it could react with lignin in a similar way to the condensation of formaldehyde with lignin (Faris *et al.* 2017). Many studies have investigated bio-based wood adhesives by producing lignin-phenol-glyoxal resins (Hussin *et al*. 2019; Younesi-Kordkheili 2019). Younesi-Kordkheili (2019) used ionic liquid treated lignin in the preparation of lignin phenol glyoxal adhesive to bond particleboard panels, which demonstrated mechanical properties in par with panels treated with phenol formaldehyde resins. As well, Hussin *et al.* (2019) obtained lignin from kenaf core (*Hibiscus cannabinus*), and partially substituted phenol in lignin-phenol-glyoxal adhesives. It was a 3:7 ratio of lignin to phenol in lignin-phenol-glyoxal resins that gave the highest internal bonding (53.83 MPa) and tensile strength (72.08 MPa) compared to that of phenol formaldehyde resin.

There have been a great number of studies regarding lignin and glyoxal utilization in wood adhesives, including the study of the preparation kraft lignin phenol glyoxal (KLPG) and soda lignin phenol glyoxal (SLPG) adhesives. However, to the best of our knowledge, the adhesives were not modified by date palm fronds lignin. In this paper, lignin was extracted from date palm fronds by the use of alkaline pulping processes (kraft and soda). Subsequently, kraft lignin (KL) and soda lignin (SL) were used to prepare both adhesives, kraft lignin phenol glyoxal and also soda lignin phenol glyoxal adhesives. Complementary analyses, Fourier transform infrared (FTIR), ^{13}C nuclear magnetic resonance (NMR), thermogravimetric analysis (TGA), and differential scanning calorimetry (DSC) were done to characterize KL and SL. Additionally, LPG adhesives' mechanical properties were studied and compared to phenol formaldehyde adhesives.

EXPERIMENTAL

Materials

The fronds of the date palm tree were sourced from Abu Dhabi, UAE in December 2018. The fronds were cut, ground, and sieved to get a fine powder. The utilized chemicals were glacial acetic acid (99.8%), formaldehyde (37%), sodium hydroxide (97%), sulphuric acid (98%), ethanol (99.7%), hydrochloric acid (37% v/v), and toluene (grade AR). These were procured from QReC, Rawang, Malaysia. Phenol (99.5%) and sodium sulphide (95%) were gained from R&M Chemical, Essex, UK. Acetic anhydride (≥ 98.5%) and glyoxal (40% wt% solution in water) were purchased from Merck, Darmstadt, Germany. Chloroform (99.8%) and tetrahydrofuran (99.99%) were purchased from Fisher Chemicals, Loughborough, UK. Sodium chlorite (80%) pure was purchased from Acros Organics, Morris Plains, NJ, USA. Pyridine (≥ 99.5%) was purchased from Bendosen, KL, Malaysia. Finally, distilled water was used in the study.

The proximate analysis for DPF was performed according to Laboratory Analytical Procedure (LAP), TAPPI T203 cm-09 (2009), and TAPPI T222 om-02 (2006), to analyze the DPF (%w/w) components in terms of the content of moisture which was 8.36 ± 0.55%, the content of ash 3.28 ± 0.82%, extractives content 0.9 ± 0.18%, cellulose 41 ± 1.00%, hemicellulose 22.8 ± 1.2%, and Klason lignin 24 ± 0.01%.

Kraft and Soda Lignin Extraction

The alkaline pulping processes were conducted in a 1.0-L high pressure reactor. The conditions for soda and kraft pulping followed the work of Hussin *et al*. (2013) with minor adjustments. The conditions used in kraft pulping were as follows: 70% of active alkali and 30% sulfidity. These were added to a solid to liquid ratio of 1:10 at 150 °C for 4 h. While in soda lignin pulping, 30% (w/v) of NaOH was used with the similar ratio, temperature, and time as kraft pulping. The pressure in both pulping processes was around 10 bar. To recover the black liquor, vacuum filtration was performed; then, 20% (v/v) sulphuric acid was used to acidify the liquor until it reached pH 2 to precipitate soda and kraft lignin (Ibrahim *et al*. 2011) The mixture was centrifuged for 20 min for further precipitation. Afterward, lignin precipitate was dried in a 50 °C oven overnight to be recovered. Lignin was added to pH 2 water for further separation of hemicellulose, then filtered and dried. Lignin yield was calculated using Eq. 1:

$$\% \text{ Yield} = \frac{weight\ of\ lignin\ recovered\ (g)}{weight\ of\ DPF\ (g)} \times 100\% \quad (1)$$

Adhesive Preparation

According to Hussin *et al*. (2018), Phenol was substituted by lignin using different percentages. The adhesive preparation method and the amounts of chemicals used were as follows; phenol formaldehyde and phenol glyoxal that contain 0 wt% of lignin were prepared as control adhesives. Meanwhile, 10, 30, and 50% wt% of phenol were substituted by both KL and SL in lignin phenol glyoxal resins. Lignin, phenol, NaOH, and ethanol amounts are summarized in Table 1. Glyoxal to phenol (G/P) molar ratio was 1.5:1.0. Ethanol was introduced as a solvent, while NaOH was added as a catalyst in the amount of 5 wt% of phenol. The mixture of lignin/formaldehyde, phenol, NaOH, and ethanol was heated under reflux with constant stirring until it reached 80 °C. Then the glyoxal was

introduced to the refluxed mixture (dropwise). The refluxed time was 2 h. After that, a rotary evaporation for the resin was performed to get rid of the excess ethanol.

Table 1. Composition Used in Resinification of Lignin Samples

Resin	Lignin (g)	Phenol (g)	Glyoxal (mL)	NaOH (g)	Ethanol (mL)	Formaldehyde (mL)
PG	-	27.46	50	1.58	100	-
PF	-	31.53	-	1.58	100	50
10% KLPG	2.746	24.71	50	1.58	100	-
30% KLPG	8.23	19.22	50	1.58	100	-
50% KLPG	13.73	13.73	50	1.58	100	-
10% SLPG	2.74	24.71	50	1.58	100	-
30% SLPG	8.23	19.22	50	1.58	100	-
50% SLPG	13.73	13.73	50	1.58	100	-

Characterizations

FTIR spectroscopy analysis

The FTIR analysis was conducted for KL, SL, and the solid adhesives using PerkinElmer System 2000 FTIR spectrometer (Waltham, MA, USA). The range of wavenumber used was from 4000 to 400 cm^{-1} and the number of scans was 20. Potassium bromide disc technique was performed in the preparation of samples with 1:100 ratio.

^{13}C NMR spectroscopy analysis

The 150 mg acetylated samples of KL and SL were dissolved in a 0.4 mL d6-DMSO with slight heating until it completely dissolved. This was used to perform ^{13}C analysis using Bruker Avance 500 NMR spectrometer (Fallanden, Switzerland) at 12000 scans at room temperature. The Bruker Top Spin software (v.3.5, Oxford, UK) was utilized to obtain and interpret the spectra.

TGA

The KL, SL, and the solid adhesives' thermal performance were studied using PerkinElmer TGA model STA 8000 (Waltham, MA, USA), the range of temperature was (30 to 900 °C) in the nitrogen atmosphere.

DSC

The KL and SL samples' glass transition temperature (T_g) was investigated *via* DSC analysis. The analysis was controlled with a heating rate of 20 °C min^{-1}, from 0 to 300 °C then cooling to 0 °C. The DSC analysis was conducted using a Q200 Differential Scanning Calorimeter from TA Instruments (New castle, DE, USA) in the School of Industrial Technology.

Physicochemical tests

The resins' physicochemical properties were tested in terms of solid content, viscosity, and gel time. The resins' viscosity was obtained using Brookfield DVII+Viscometer (Middleborough, MA, USA), spindle No. 5 with 100 rpm at room temperature. The recorded viscosity was in Pascal-second (Pa-s) units (Hussin *et al*. 2018) For the solid content determination, around 1.0 g of each resin was placed in a petri dish, which was placed in 105 °C oven for 24 h as the standard method of TAPPI T650 cm-15 (2015). The nonvolatile content was determined using Eq. 2:

$$\% \text{ Solid content} = \frac{\text{Final weight}}{\text{Initial weight}} \times 100\% \quad (2)$$

Additionally, the resins' gel time was determined by placing approximately 1.5 g of each resin in a 17-mm test tube. Then, the tube was heated in an oil bath at 140 °C. The resins were stirred with a helical copper coil until gelation. The gel time was recorded in seconds (s) (Hussin *et al*. 2018).

Curing of LPG Adhesives to Plywood

Resins were spread over three layers of veneer wood and pressed two times in a hot-press machine (Carver, Wabash, IN, USA). First, each specimen was pressed at room temperature for 7 min. Second, the wood panels were pressed at 140 °C for another 7 min. The pressure used in both pressing times was 1.4479×10^7 Pa. The pressing method was in accordance with the Japanese Industrial Standards, JIS- A 5908 (2003). Particleboards.

Mechanical Test

For the mechanical performance of the wood adhesives, the wood panels were cut in the dimensions of 12.0 cm × 2.0 cm × 0.6 cm. The tensile strength test was conducted in dry condition. The test was conducted using Instron UTM 5582 (Instron, Norwood, MA, USA) in the School of Industrial Technology, USM (Malaysia).

RESULTS AND DISCUSSION

Table 2 summarizes the proximate and elemental analyses results of lignin. The results showed that the soda lignin had a higher yield than the kraft lignin as a result of the higher severity of the reaction conditions. The presence of nitrogen in each lignin was probably because of the amino acid (protein building blocks) base of forming the monolignols and the crosslinking of lignin to hemicellulose *via* a cell wall protein (Horwath 2015). Thus, as nitrogen is a component of amino acids, a trace amount will be present in lignin. The presence of protein attached to lignin in a small amount proposes the stable chemical bond that is hard to break despite acid precipitation, as many studies previously have revealed (Hussin *et al*. 2013).

Table 2. Proximate Analysis of Kraft and Soda Lignin from Date Palm Fronds

	Kraft Lignin	Soda Lignin
Yield (%)	17 ± 0.2	21 ± 0.1
Element (%)		
Carbon	62.47	57.48
Hydrogen	4.62	5.06
Nitrogen	0.52	0.51
Oxygen	32.39	36.95
Double Bond Equivalent (DBE)	6.03	5.28

FTIR Analysis

Date palm fronds' KL and SL FTIR spectra are represented in Fig. 1. The spectra showed the characteristic bands for syringyl (S) and guaiacyl (G) in the region of 1450 to 800 cm^{-1}.

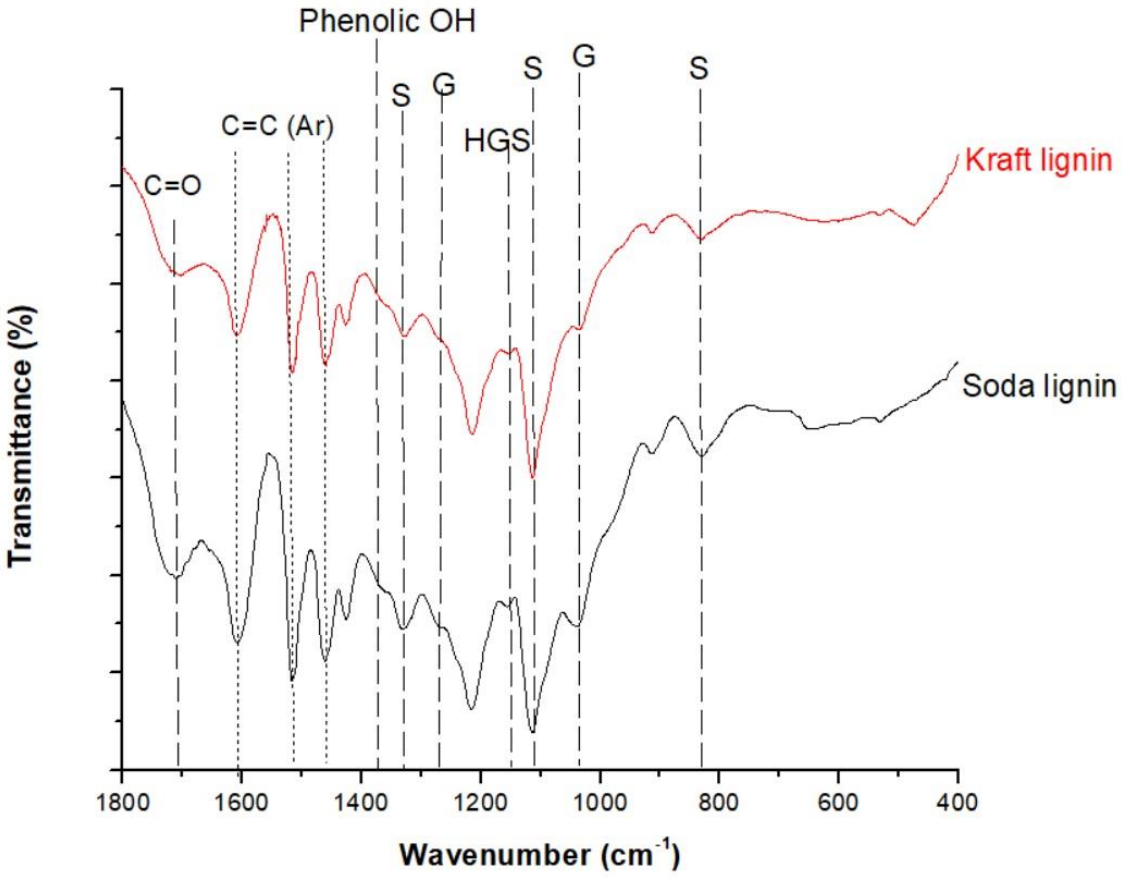

Fig. 1. FTIR spectra of the expanded spectrum between 1800 to 400 cm^{-1} for DPF lignin

Table 3. Assignment of FTIR Spectra for Date Palm Fronds Lignin

Assignment	Kraft Lignin	Soda Lignin
	Band Location (cm^{-1})	
O-H (phenolic and aliphatic) stretching	3414	3405
C-H stretching (CH3 and CH2 groups)	2939	2937
C–H stretching (OCH3)	2851	2847
C=O stretching (unconjugated ketone, carbonyl, and ester groups)	1715	1714
C=C stretching (aromatic skeleton)	1610, 1516	1612, 1518
C-H deformation (asymmetric in $-CH_3$ and $-CH_2$)	1463	1463
C-C stretching (aromatic skeleton) with C-H in plane deformation	1427	1426
C-O stretching (syringyl)	1331	1334
O-H (phenolic) In-plane deformation vibration	1365	1365
C–O stretching vibration of secondary alcohol	1275	1273
C-O (H) + C-O (Ar) (phenolic OH and ether in syringyl and guaiacyl)	1216	1217
Ar-CH in plane deformation (syringyl)	1116	1114
C-O (H) + C-O (C) (first order aliphatic OH and ether	1064	1044
C-H out of plane (aromatic ring)	953	918
C-H out of plane (aromatic ring)	835	829

Table 3 represents the assignments of the corresponding bands. Both lignin samples showed low absorbance intensity for G bands (~1044 and 1273 cm^{-1}) and modest to high absorbance intensity for S bands (~830, 1115, and 1330 cm^{-1}), which suggests higher syringyl content in lignin. It is believed that different pulping process will give different absorbance intensity (Thring *et al.* 1990). The S bands appeared as less intense peaks in KL than SL owing to the demethoxylation during the kraft pulping process (Nadji *et al.* 2009; Hussin *et al*. 2013). The severe conditions of kraft pulping process converts S-type units into more stable G-type units. According to the FTIR spectra, the results confirmed the presence of potential active sites for lignin polymerization due to the presence of G-type units.

^{13}C NMR Analysis

The ^{13}C NMR characterization was performed for further investigation of the isolated lignin structures. Figure 2 illustrates the ^{13}C NMR spectra for the acetylated KL and SL. The KL and SL samples were introduced into acetylation process according to Váquez-Torres *et al*. (1992), to improve their solubility in organic solvents. Acetyl groups became as a substituent to all the hydroxyl functional groups *via* the acetylation reaction. The region between 104 to 154 ppm represented the signals of S, G, and p-hydroxyphenyl (H) units (Fig. 2b) as follows; 104 ppm (C2/C6,S), 139 ppm (C4,S), 152 ppm (C3/C5, S etherified), 148.5 ppm (C3/C5,S non-etherified), 114 ppm (C2,G), 116 ppm (C5,G), 120 ppm (C6,G), 134 ppm (C1,G etherified), 145 ppm (C3,G non-etherified), and 127.4 ppm is for (C2/C6, p-coumaric acid ester). The aliphatic esters and aliphatic carboxyls appeared around 170 ppm, relating to lignin oxidation during alkaline pulping (Sun *et al*. 2012). While the strong signal at 56.5 ppm represented the methoxyl group in both the S and G units.

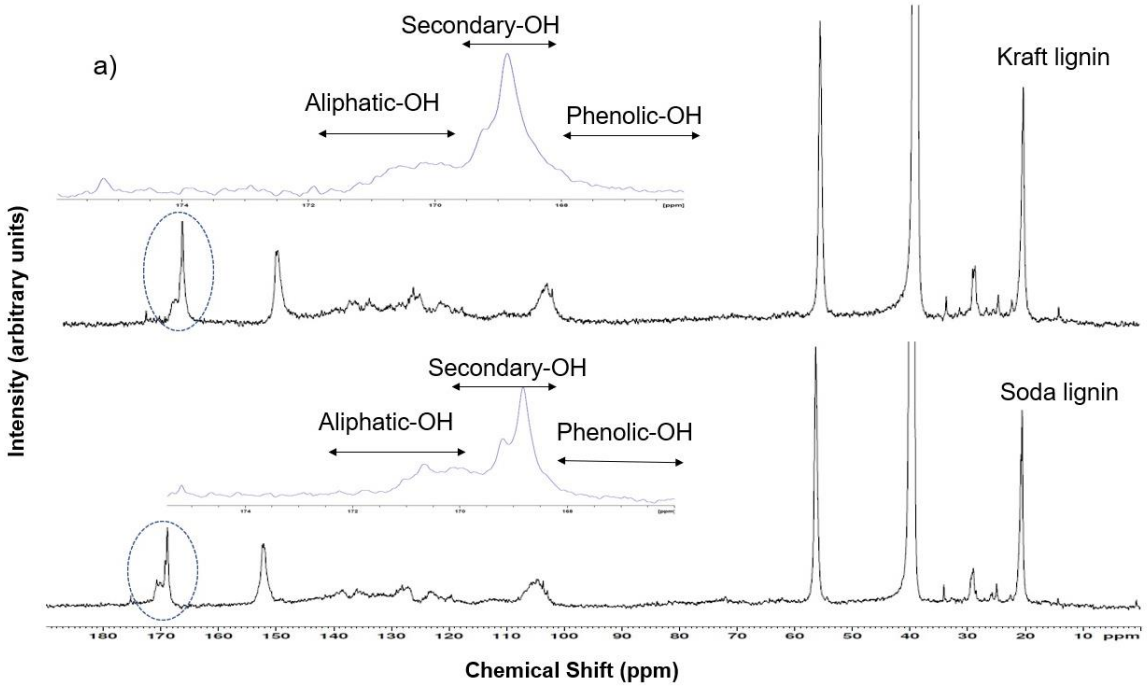

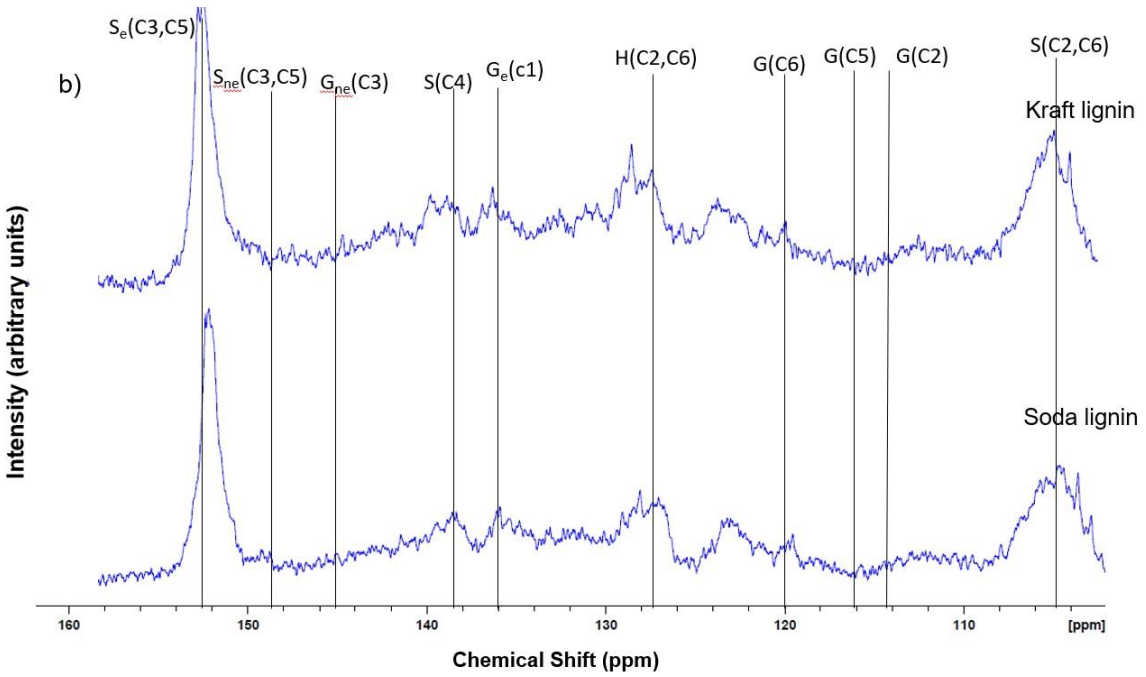

Fig. 2. ^{13}C NMR spectra of (a) acetylated DPF lignin with (b) expanded aromatic region; H: p-hydroxyphenyl unit; G: guaiacyl unit; S: syringyl unit; e: etherified; ne: non etherified

The integral region of 162 to 102 ppm was established as a reference, as the presumption is that it consists of six aromatic carbons and 0.12 vinylic carbons. Thus, the integral values in that region were divided by 6.12 to be equivalent to one aromatic ring (Ar), with the aim of studying the quantity of each hydroxyl groups per one aromatic ring (Capanema *et al*. 2004).

Table 4 shows the region between 172 to 166 ppm, in which KL had higher phenolic-OH amount (1.4/Ar) than SL (0.9/Ar). Furthermore, the quantity of secondary-OH in KL was 2.0/Ar, which was higher than SL (1.6/Ar). Meanwhile, the quantity of aliphatic-OH was almost constant for KL (1.3/Ar) and SL (1.4/Ar). It was clear that the ratio of aromatic to aliphatic hydroxyls was alike for both KL and SL, due to the effect of the pulping method: kraft pulping generates phenolic-OH through the bond of aryl-ether cleavage in DPF and lignin depolymerization, while soda pulping eliminates aliphatic-OH (Tejado *et al*. 2007). Thus, that explains the higher phenolic-OH amount in KL, which leads to a higher amount of aromatic ring positions for the cross-linking with glyoxal through the resinification process.

Table 4. Comparison of the Hydroxyl and Methoxy Groups Amount Between Acetylated Kraft and Soda Lignin from Date Palm Fronds

Range (ppm)	Assignment	Amount (Per Aromatic)	
		Kraft Lignin	Soda Lignin
172 to 169.6	Aliphatic-OH	1.3	1.4
169.6 to 168.6	Secondary-OH	2.0	1.6
168.6 to 166	Phenolic-OH	1.4	0.9
58 to 54	Methoxy group (–OCH_3)	4.7	4.6

Thermal Analysis

TGA

Thermogravimetric study was conducted to investigate the thermal behavior of DPF lignin. Figure 3 (a and b) illustrated the thermogravimetric (TG) and differential thermogravimetric (DTG) curves of KL and SL, respectively. The curves show that the range of thermal degradation temperature was between 100 and 900 °C.

It can be seen from Fig. 3a that, around 53 °C, a weight loss for both lignin samples occurred due to attached and absorbed water evaporation that generates carbon dioxide and methane, side unsaturated chains, and carbon monoxide (Hoareau *et al*. 2004). The next phase of weight loss was around 209 to 243 °C due to degradation of carbohydrates. Xylose degrades when the temperature increased from 200 to 270 °C (Sahoo *et al*. 2011). In addition, it was found by García *et al*. (2009) that the attached hemicellulose to lignin degrades at 200 to 300 °C.

Above 300 °C, lignin structures started to degrade, mainly through the cleavage of methyl-aryl ether bonds that liberated water and formaldehyde (Sun *et al*. 2000; Tejado *et al*. 2007) until the maximum rate of weight loss (DTG_{max}) at 375 °C and 381 °C for KL and SL, respectively (Fig. 3b).

It was noticed that SL had higher thermal degradation compared to KL as the temperature was raised from 380 to 450 °C, which could be due to a high purity and large number of $–OCH_3$ groups (Sahoo *et al*. 2011). The DPF lignin was compared to lignin from oil palm empty fruit bunch (Ibrahim *et al*. 2011) and from corn cob (Ibrahim *et al*. 2010), DTG_{max} around 347 °C and 352 °C, respectively.

The DPF lignin has higher DTG_{max}, indicating a higher thermal stability and higher cross-linking. The non-volatile components for KL and SL were 61% and 51%, respectively. The higher residue for KL revealed that it has a higher content of inorganic material, probably form the addition of sodium sulphide in kraft pulping process (Hussin *et al.* 2019).

The narrow curve in Fig. 3b for both lignin samples suggested a high cross-linked structure and more C-C interlinked bonds (Hussin *et al.* 2013). This result was also supported by the high residue percentages for both lignin samples. The thermal analysis results showed that KL and SL samples from DPF were steady at elevated temperature, which reveals a high branching degree and high condensed aromatic structure.

DSC

The DSC study was conducted to correlate glass transition temperature (T_g) to the molecular weight of lignin samples. The result showed that SL's T_g value was 40.4 °C, which was greater than KL's T_g value (T_g = 36.57 °C). Theoretically, the T_g value describes the ability of the main chain of the polymer to rotate in terms of the obtained energy. At first, the chains in the lignin molecule received energy to vibrate, then to rotate as it receives more energy.

As a result, T_g can be correlated to the molecular weight based on the free volume in the molecule (Thring *et al.* 1991). In this case, SL had higher molecular weight, which suggests that it had few chain ends that lead to a low volume movement that entails further energy to pivot the chain and higher T_g value (Ibrahim *et al*. 2011).

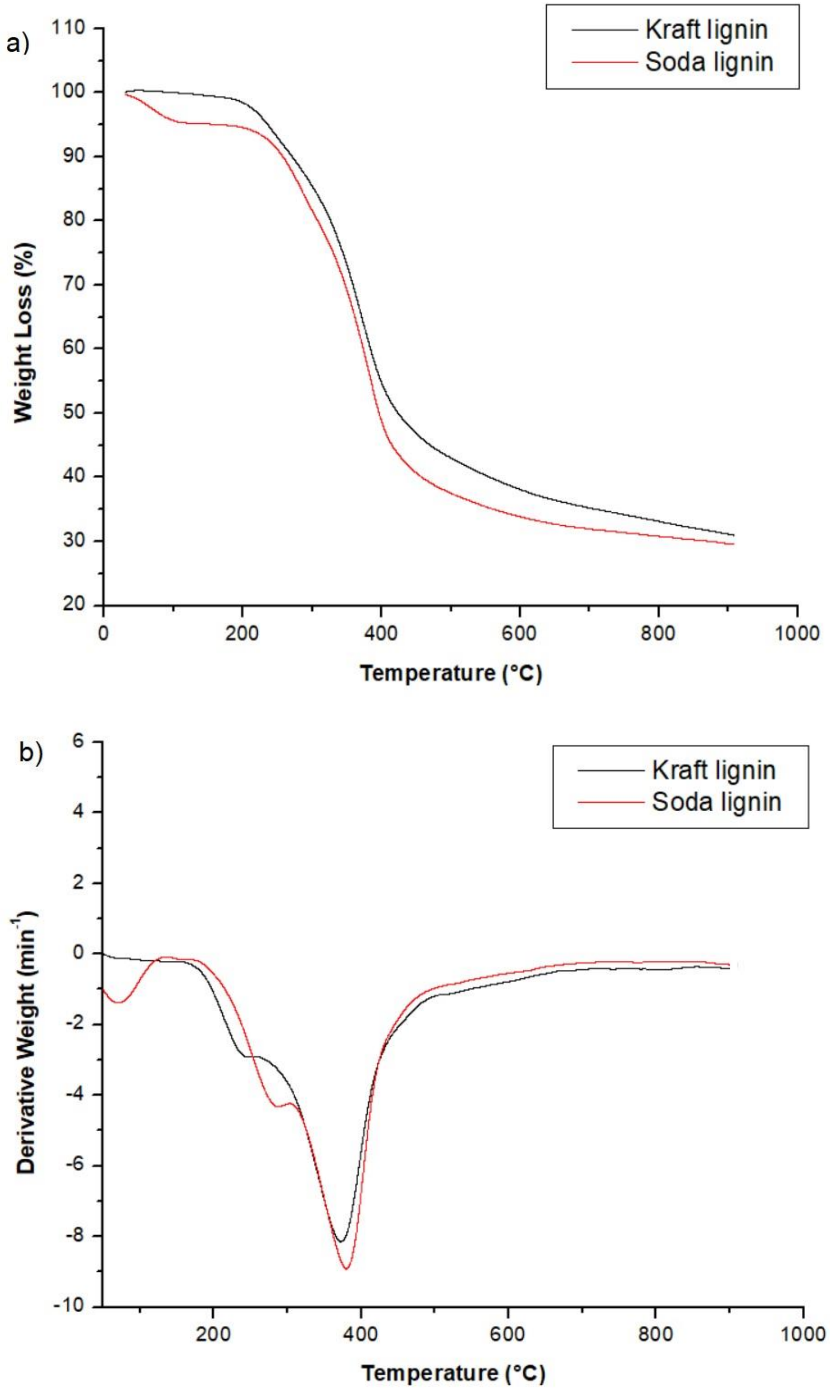

Fig. 3. a) TG and b) DTG curves of DPF lignin

Characterization of Wood Adhesives

Table 5 shows the solid content, viscosity, and gel time for LPG resins, PG, and PF resins. The results for solid content showed an increment as the phenol percent substitution with lignin increased. The substitution of 50% KPLG had the highest solid content (50% KLPG: 40%) but PG resins with zero lignin substitution had the lowest solid content percentage (PG: 23.5%). As for SLPG resins, it showed the same trend for solid content (10% SLPG: 32.0 < 30% SLPG: 35.5% < 50% SLPG: 37.0%).

Table 5. Solid Content, Viscosity, and Gel Time for Control Resins (Phenol Formaldehyde (PF) and Phenol Glyoxal (PG)), Soda Lignin Phenol Glyoxal (SLPG), and Kraft Lignin Phenol Glyoxal (KLPG)

Resin	Solid Content (%)	Viscosity (Pa-s)	Gel Time (s)
PF	60.0	0.192 ± 1.5	100
PG	23.5	0.036 ± 4.0	660
10% SLPG	32.0	0.045 ± 2.3	295
30% SLPG	35.5	0.091 ± 3.0	231
50% SLPG	37.0	0.110 ± 5.0	150
10% KLPG	31.0	0.046 ± 2.3	280
30% KLPG	36.0	0.092 ± 2.5	240
50% KLPG	40.0	0.165 ± 2.8	140

Note: Solid content is the nonvolatile content of the resin, viscosity is the thickness of the resin, gel time is the time it takes for a resin to become so highly viscous

In the same way, the increase in lignin substitution increased the viscosity value for LPG adhesives. In this study, as the amount of lignin increased from 10% to 50% in KLPG, the viscosity surged from 0.046 to 0.165 Pa-s. The same trend was seen in SLPG viscosity values compared to PG resin (PG: 0.036 Pa-s < 10% SLPG: 0.045 Pa-s < 30% SLPG: 0.091 Pa-s < 50% SLPG: 0.106 Pa-s). It was believed that the viscosity would indicate the degree of condensation; therefore, the higher amount of lignin will contribute to a higher amount of depolymerized lignin. This would cause the elongation of the polymeric chains or additional branching within the structure of LPG resins, which would improve their density. The resins' high density prevents their mobility and triggers rapid freezing when exposed to air (Ibrahim *et al*. 2007; Monni *et al*. 2007).

The gel time correlates with viscosity and solid content; therefore, the increase in phenol substitution amount results in faster resin gelation. The shortest gel time presented by 50% KLPG at 149 s compared to 660 s for PG (zero lignin). This result can be ascribed to the higher viscosity and solid content of 50% KLPG, which indicates its higher degree of condensation (Siddiqui 2013).

The FTIR spectra of PG, 50% SLPG, and 50% KLPG adhesives are shown in Fig. 4; the corresponding band assignments are summarized in Table 6. The results presented similar trends compared to former studies (Aziz *et al*. 2019; Hussin *et al*. 2019). The band at 1467 cm^{-1} represents the C-H deformation in the $–CH_2$ bridge in 50% KLPG and SLPG. It indicates the formulation of the connection between lignin and phenol glyoxal in the resins. Other peaks have increased or appeared after the condensation reaction, such as the band ∼1047 cm^{-1} that corresponded to C-O stretching vibration of first order aliphatic OH, C-O (methylol) and ether, which does not appear in PG spectra. The band located at ∼1200 cm^{-1} was attributed to C-C, C-O, and C=O stretching vibration as a result of introducing glyoxal into lignin structure through the condensation procedure (El Mansouri *et al*. 2011). The C-O stretching in phenolic OH and ether in S and G type is represented by the peak 1218 cm^{-1}. According to the resins' FTIR spectra, the presence of G-type units and phenolic hydroxyl groups in LPG make it suitable to form a lignin-based wood adhesive.

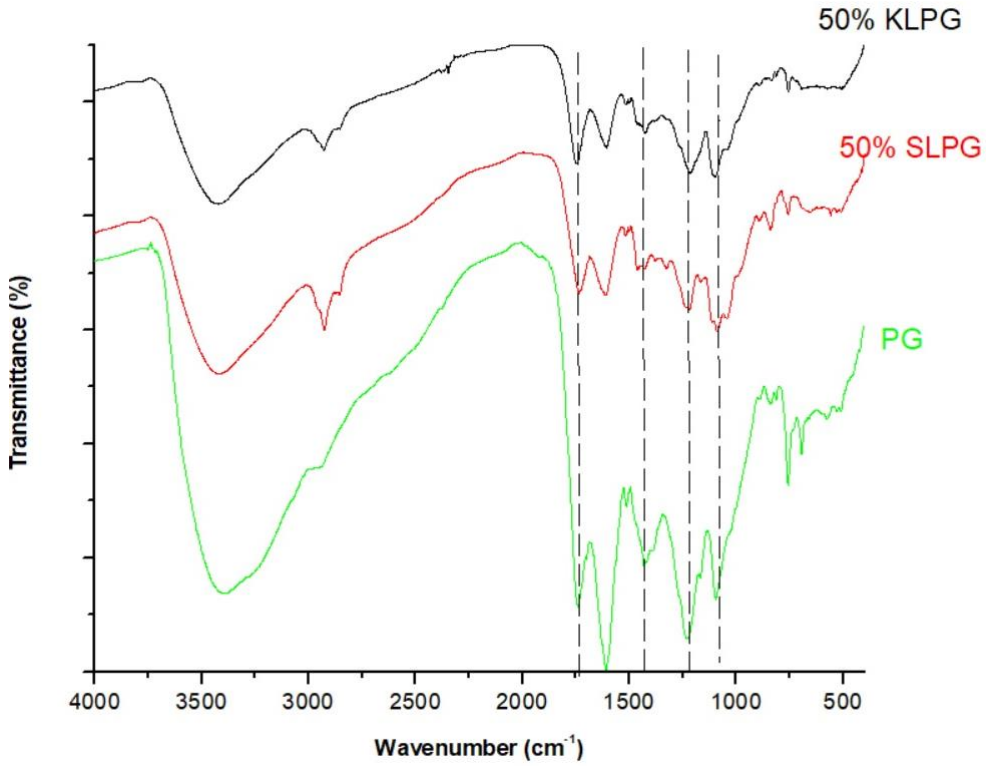

Fig. 4. FTIR spectra of KLPG, SLPG, and PG

Table 6. Band Assignment for FTIR Spectra of PG, KLPG, and SLPG Resins

Assignments	PG	KLPG	SLPG
	Wavenumber (cm^{-1})		
OH stretching vibration	3425	3440	3439
Asymmetric CH2 vibration	2961	2930	2929
C=O stretching of aldehyde/ketone groups	1741	1751	1734
C=C stretching vibration in benzene ring	1613	1611	1617
C-H deformation mode in CH_2 groups (-CH_2 bridge)	-	1467	1467
C-C stretching (aromatic skeleton) with C-H in plane deformation	1400	-	-
C-O stretching (syringyl)	-	1342	1335
C-O(H) + C-O(Ar) (phenolic OH and ether in syringyl and guaicyl	1238	1218	1223
C-O(H) + C-O(C) (first order aliphatic OH and ether)	-	1043	1047
C-H out of plane (aromatic)	849	836	846
C-H out of plane, para-substituted	833	816	825
C-H out of plane, ortho-substituted	760	757	763
Adjacent 5H	695	697	669

The ^{13}C NMR spectra (Fig. 5) showed noticeable peaks that resulted from the lignin phenol glyoxal resinification process. Mainly, the methylol group peak (–CH_2OH) appeared at 64 ppm. This correlated with the benzyl alcohol group that was produced due to glyoxalation and attached to the ortho site of the aromatic ring. As a result, a quinone methide and a phenoxy group also formed and showed a peak at around 174 and 158 ppm, respectively (Mansouri *et al*. 2007). The peaks that correspond to phenolic-OH disappeared as a result of introducing the hydroxymethyl groups on C3 and C5 positions in the aromatic ring of lignin, which was supported by the appearance of methylol peaks. A signal around 57 ppm illustrated the shift of the carbon on the methoxy group (–OCH_3), which was attributed to G and S units in kraft and soda lignin. Moreover, the peak at around 90 ppm corresponded to glyoxal oligomers. The region between 130 and 110 ppm represented the substituted ortho and para carbon positions on the aromatic ring (Trosa and Pizzi 1998). The aromatic carbons peaks demonstrate the polymerization of lignin and phenol, which could give the intense peaks at aromatic position.

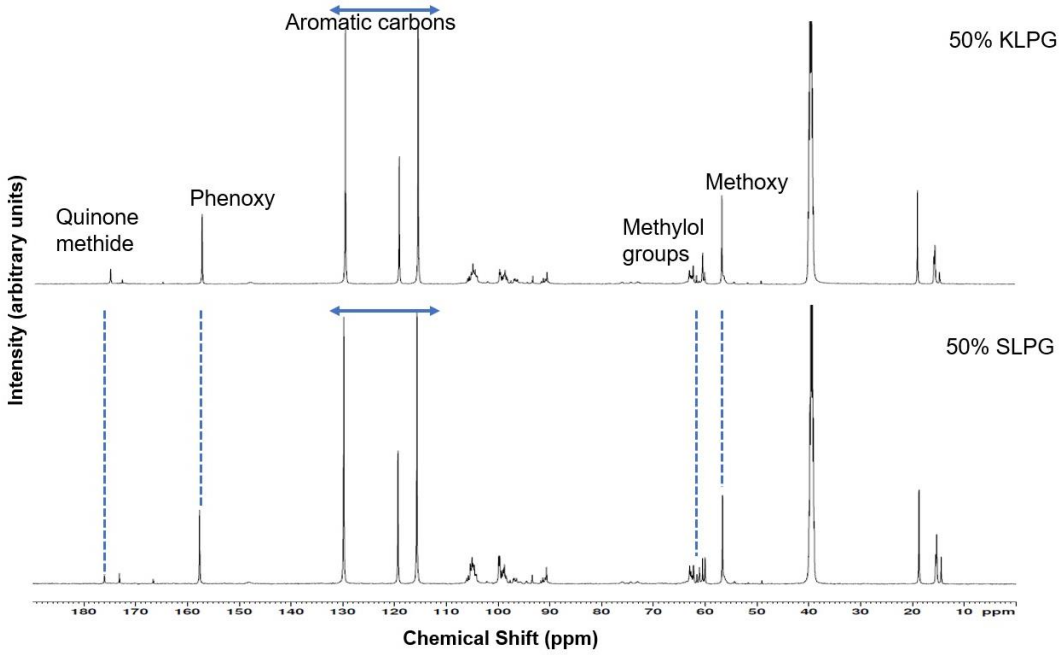

Fig. 5. ^{3}C NMR spectra of 50% KLPG and 50% SLPG adhesives

The thermal behavior of LPG and PG resins was investigated by TGA analysis. The results were compared to previous studies, and most of the lignocellulosic materials showed the same trend (Ramires *et al*. 2010; Wang *et al*. 2018; Hussin *et al*. 2019). From the curves (Fig. 6), a slight weight loss was observed below 120 °C as a result of free water evaporation and other small volatile molecules. Between 200 and 300 °C, the weight loss was due to the water evaporation, glyoxal, and phenol – which were founded as a result of the condensation of methylol groups – were observed due to evaporation. Additionally, the water that was established by the condensation of the methylene groups and the phenolic-OH caused the weight loss at around 350 to 450 °C. The last thermal degradation between 450 and 600 °C was due to the loss of carbon monoxide and methane that were found by the reaction between water and the hydrogen with methylene groups, respectively (Trick and Saliba 1995; Lenghaus *et al*. 2001).

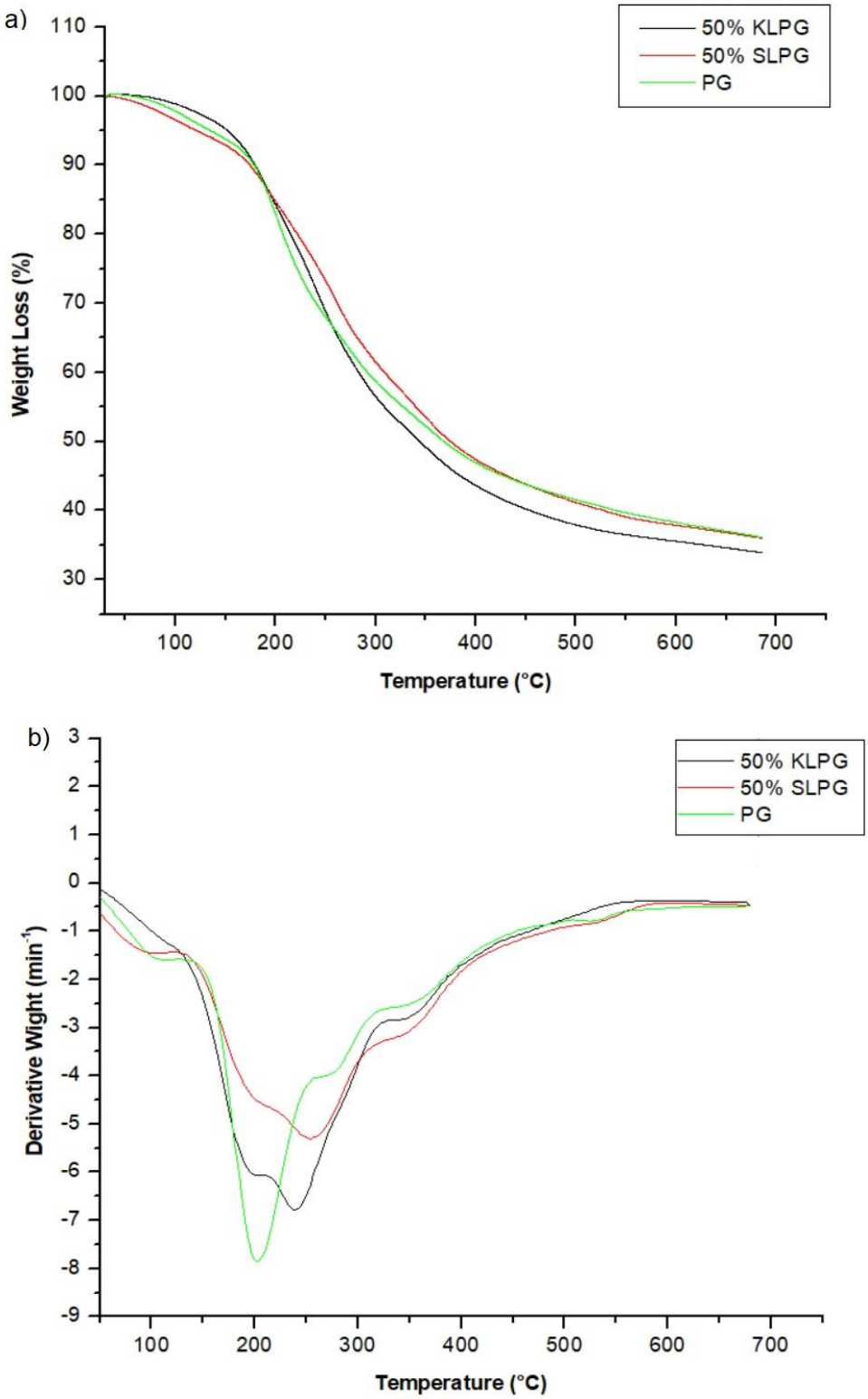

Fig. 6. a) TG and b) DTG curves of 50% KLPG, 50% SLPG, and PG resins

From Fig. 6b, it is clear that DTG_{max} increased from 204 °C for PG to 242 °C and 258 °C for 50% KLPG and SLPG, respectively. The results suggested an improvement to the thermal performance of LPG due to the cross-linking between lignin and glyoxal, which increased the molecular weight of lignin. In addition, the decomposition rate reduced for LPG resins compared to PG, which could be due to the reaction degree variation for cross-linking with glyoxal (Wang *et al.* 2018). The residue of KLPG and SLPG samples at around 600 °C were 17.4% and 20.3%, respectively, which are lower than the residue of PG (28.6%). This can be ascribed to the free volume in LPG that leads to a full degradation. This could be attributed to the increase of the side chain on C3 and C5 positions due to glyoxal addition (Glasser and Jain 1993; Wang *et al*. 2018).

Physico-mechanical Analysis of Wood Adhesives

At replacement levels from 10 up to 50% kraft and soda lignin (10%, 30%, and 50% LPG), the mechanical strength were equal or higher than the commercial resin PF. The highest tensile strength (65.3 MPa), elastic modulus (581.3 MPa), and elongation at break (15.5%) were represented by 50% KLPG. In contrast, the commercial resin (PF) recorded lower mechanical properties values than 50% KLPG (tensile strength: 58.6 MPa, elastic modulus: MPa, and elongation at break: 13.1%) (Table 7).

Table 7. Physico-mechanical Analysis of PG, PF, KLPG, and SLPG Adhesives

Resin	Tensile Strength (MPa)	Elastic Modulus (MPa)	Elongation at Break (%)
PF	58.57 ± 0.91	551.43 ± 1.07	13.14 ± 0.51
PG	63.53 ± 0.78	604.68 ± 1.10	12.68 ± 0.03
10% SLPG	43.36 ± 1.01	427.16 ± 1.21	13.41 ± 1.02
30% SLPG	54.94 ± 1.22	530.13 ± 1.02	14.46 ± 0.70
50% SLPG	61.02 ± 0.75	532.18 ± 0.95	15.74 ± 0.32
10% KLPG	58.34 ± 0.98	501.65 ± 1.06	14.57 ± 0.21
30% KLPG	59.63 ± 1.02	565.86 ± 1.12	14.26 ± 1.01
50% KLPG	65.30 ± 0.88	581.32 ± 0.87	15.46 ± 0.34

It was clear that at 50% kraft lignin substitution, the cross-linking formation was at the highest level. This may be due to the presence of phenolic-OH in lignin molecules. As a result, KL effectively substituted for phenol in LPG resins, while glyoxal was able to entirely substitute for formaldehyde (Hussin *et al*. 2018). From the results illustrated in Fig. 7, 50% KLPG has the highest tensile strength due to the highest amount of phenolic groups as reported in ^{13}C NMR analysis. Lignin-phenol-glyoxal condensation takes place through electrophilic substitution of glyoxal in G-type lignin-free sites (C5 and C3 positions). Furthermore, the high amount of phenolic-OH groups in the structure of lignin provides active positions at the aromatic ring for glyoxal reaction (Thring *et al.* 1990; Tejado *et al*. 2007). The relatively higher amount of phenolic-OH in kraft lignin compared to soda lignin indicates the higher amount of aromatic rings. As a result, during the condensation reaction, the molecular weight, solid content, and viscosity of the resol resin increase so that they can be used as wood adhesive, as shown in the physico-chemical results. During the curing process, methylol groups are transformed from low molecular weight materials into a highly branched network of LPG resin using temperature around 140 °C. The structure of the resin in this stage is more complex resulting from additional condensation reaction (Siddiqui 2013).

Overall, 50% KLPG demonstrated durable bonding characteristics in comparison to the commercial PF adhesives. The 50% KLPG adhesive showed that it is possible to produce an ecofriendly wood adhesive from date palm fronds lignin and glyoxal as phenol and formaldehyde substituents, respectively.

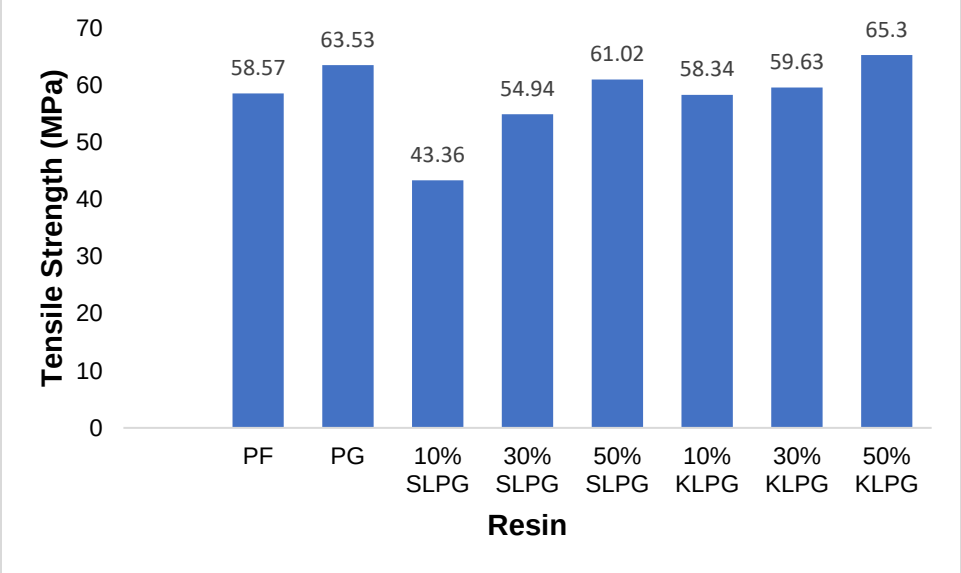

Fig. 7. Tensile strength of PG, LPG, and PF adhesives

CONCLUSIONS

1. The characteristics of the extracted date palm fronds' lignin demonstrated that both kraft and soda lignin can serve as a partial substituent of phenol in lignin phenol glyoxal resins
2. Kraft and soda lignin from date palm fronds (DPF) demonstrated thermal stability, showing that the maximum of the differential thermogravimetric (DTG_{max}) curve for kraft and soda lignin was 375 and 381 °C, respectively.
3. In terms of physicochemical properties, 50% kraft lignin phenol glyoxal (KLPG) adhesive presented the highest solid content (40%), viscosity (0.165 Pa-s), and the shortest gel time (140 s) in comparison with 50% soda lignin phenol glyoxal (SLPG) and phenol glyoxal (PG) resins.
4. The physico-mechanical properties showed that 50% KLPG resin has the highest tensile strength in dry conditions (65.30 MPa) compared to SLPG and PF resins. In conclusion, 50% KLPG resin can substitute the commercial PF adhesives as a stronger and non-toxic green wood adhesive.

ACKNOWLEDGMENTS

This work was supported by Universiti Sains Malaysia (Penang, Malaysia) through USM Research University Incentive Grant – 1001/PKIMIA/8011077.

REFERENCES CITED

Aziz, N. A., Latip, A. F. A., Peng, L. C., Latif, N. H. A., Brosse, N., Hashim, R., and Hussin, M. H. (2019). "Reinforced lignin-phenol-glyoxal (LPG) wood adhesives from coconut husk," *Int. J. Biol. Macromol*. 141, 185-196. DOI: 10.1016/j.ijbiomac.2019.08.255

Ballerini, A., Despres, A., and Pizzi, A. (2005). "Non-toxic, zero emission tannin-glyoxal adhesives for wood panels," *Holz. Roh. Werkst*. 63(6), 477-478. DOI: 10.1007/s00107-005-0048-x

Capanema, E. A., Balakshin, M., and Kadla, J. (2004). "A comprehensive approach for quantitative lignin characterization by NMR spectroscopy," *J. Agr. Food Chem.* 52(7), 1850-1860. DOI: 10.1021/jf035282b

Danielson, B., and Simonson, R. (1998). "Kraft lignin in phenol resin. Part 1. Partial replacement of phenol by kraft lignin in phenol formaldehyde adhesives for plywood," *J. Adhes. Sci. Technol.* 12(9), 923-939. DOI: 10.1163/156856198X00542

El Mansouri, N. E., Yuan, Q., and Huang, F. (2011). "Study of chemical modification of alkaline lignin by the glyoxalation reaction," *BioResources* 6(4), 4523-4536.

Faris, A. H., Rahim, A. A., Ibrahim, M. N. M., Hussin, M. H., Alkurdi, A. M., and Salehabadi, A. (2017). "Investigation of oil palm based kraft and auto-catalyzed organosolv lignin susceptibility as a green wood adhesives," *Int. J. Adhes. Adhes*. 74, 115-122. DOI: 10.1016/j.ijadhadh.2017.01.006

Foyer, G., Chanfi, B. H., Virieux, D., David, G., and Caillol, S. (2016a). "Aromatic dialdehyde precursors from lignin derivatives for the synthesis of formaldehyde-free and high char yield phenolic resins," *Eur. Polym. J*. 77, 65-74. DOI: 10.1016/j.eurpolymj.2016.02.018

Foyer, G., Chanfi, B. H., Boutevin, B., Caillol, S., and David, G. (2016b). "New method for the synthesis of formaldehyde-free phenolic resins from lignin-based aldehyde precursors," *Eur. Polym. J. 74*, 296-309. DOI: 10.1016/j.eurpolymj.2015.11.036

García, A., Toledano, A., Serrano, L., Egüés, I., Alriols, M. G., Marín, F., and Labidi, J. (2009). "Characterization of lignins obtained by selective precipitation," *Sep. Purif. Technol.* 68(2), 193-198. DOI: 10.1016/j.seppur.2009.05.001

Glasser, W. G., and Jain, R. K. (1993). "Lignin derivatives. I. Alkanoates," *Holzforschung* 47(3), 225-233. DOI: 10.1515/hfsg.1993.47.3.225

Hoareau, W., Trindade, W., Siegmund, B., Castellan, A., and Frollini, E. (2004). "Sugar cane bagasse and curaua lignins oxidized by chlorine dioxide and reacted with furfuryl alcohol: Characterization and stability," *Polym. Degrad. Stabil.* 86(3), 567-576. DOI: 10.1016/j.polymdegradstab.2004.07.005

Horwath, W. (2015). "Carbon cycling: The dynamics and formation of organic matter," in: *Soil Microbiology, Ecology and Biochemistry* (4th ed.), E. A. Paul (ed.), Academic Press, Fort Collins, CO, USA.

Hussin, M. H., Rahim, A. A., Ibrahim, M. N. M., and Brosse, N. (2013). "Physicochemical characterization of alkaline and ethanol organosolv lignins from oil palm (*Elaeis guineensis*) fronds as phenol substitutes for green material applications," *Ind. Crop. Prod.* 49, 23-32. DOI: 10.1016/j.indcrop.2013.04.030

Hussin, M. H., Zhang, H. H., Aziz, N. A., Samad, N. A., Faris, A. H., Ibrahim, M. N. M., Iqbal, A., Latip, A. F. A., and Haafiz, M. K. M. (2017). "Preparation of environmental friendly phenol-formaldehyde wood adhesive modified with kenaf lignin," *J. Appl. Sci.* 6(4), 409-418. DOI: 10.1016/j.bjbas.2017.06.004

Hussin, M. H., Samad, N. A., Latif, N. H. A., Rozuli, N. A., Yusoff, S. B., Gambier, F., and Brosse, N. (2018). "Production of oil palm (*Elaeis guineensis*) fronds lignin-derived non-toxic aldehyde for eco-friendly wood adhesive," *Int. J. Biol. Macromol*. 113, 1266-1272. DOI: 10.1016/j.ijbiomac.2018.03.048

Hussin, M. H., Aziz, A. A., Iqbal, A., Ibrahim, M. N. M., and Latif, N. H. A. (2019). "Development and characterization novel bio-adhesive for wood using kenaf core (*Hibiscus cannabinus)* lignin and glyoxal," *Int. J. Biol. Macromol*. 122, 713-722. DOI: 10.1016/j.ijbiomac.2018.11.009

IARC Working Group on the Evaluation of Carcinogenic Risks to Humans (2006). *Formaldehyde, 2-Butoxyethanol and 1-Tert-butoxypropan-2-ol, IARC Monographs on the Evaluation of Carcinogenic Risks to Humans* (Vol. 88), International Agency for Research on Cancer, World Health Organization, Lyon, France.

Ibrahim, M. N. M., Ghani, A. M., and Nen, N. (2007). "Formulation of lignin phenol formaldehyde resins as a wood adhesive," *Malaysian J. Anal. Sci*. 11(1), 213-218.

Ibrahim, M. M., Agblevor, F., and El-Zawawy, W. K. (2010). "Isolation and characterization of cellulose and lignin from steam-exploded lignocellulosic biomass," *BioResources* 5(1), 397-418. DOI:10.15376/biores.5.1.397-418

Ibrahim, M. N. M., Zakaria, N., Sipaut, C. S., Sulaiman, O., and Hashim, R. (2011). "Chemical and thermal properties of lignins from oil palm biomass as a substitute for phenol in a phenol formaldehyde resin production," *Carbohyd. Polym*. 86(1), 112-119. DOI: 10.1016/j.carbpol.2011.04.018

JIS A 5908 (2003). "Particleboards," Japanese Standards Association, Tokyo, Japan.

Lenghaus, K., Qiao, G. G., and Solomon, D. H. (2001). "The effect of formaldehyde to phenol ratio on the curing and carbonisation behaviour of resole resins," *Polym. J*. 42(8), 3355-3362. DOI: 10.1016/S0032-3861(00)00710-2

Mallaki, M., and Fatehi, R. (2014). "Design of a biomass power plant for burning date palm waste to cogenerate electricity and distilled water," *Renew. Energ*. 63, 286-291. DOI: 10.1016/j.renene.2013.09.036

Mansouri, N., Pizzi, A., and Salvado, J. (2007). "Lignin-based polycondensation resins for wood adhesives," *J. Appl. Polym. Sci*. 103(3), 1690-1699. DOI: 10.1002/app.25098

McGregor, D., Bolt, H., Cogliano, V., and Richter-Reichhelm, H. B. (2006). "Formaldehyde and glutaraldehyde and nasal cytotoxicity: Case study within the context of the 2006 IPCS human framework for the analysis of a cancer mode of action for humans," *Crit. Rev. Toxicol*. 36(10), 821-835. DOI: 10.1080/10408440600977669

Monni, J., Alvila, L., and Pakkanen, T. T. (2007). "Structural and physical changes in phenol−formaldehyde resol resin, as a function of the degree of condensation of the resol solution," *Ind. Eng. Chem. Res.* 46(21), 6916-6924. DOI: 10.1021/ie070297a

Moubarik, A., Barba, F. J., and Grimi, N. (2015). "Understanding the physicochemical properties of olive kernel to be used as a potential tool in the development of phenol-formaldehyde wood adhesive," *Int. J. Adhes. Adhes.* 61, 122-126. DOI: 10.1016/j.ijadhadh.2015.06.003

Nadji, H., Diouf, N., Benaboura, A., Bedard, Y., Riedl, B., and Stevanovic, T. (2009). "Comparative study of lignins isolated from Alfa grass (*Stipa tenacissima* L.)," *Bioresource Technol.* 100(14), 3585-3592. DOI: 10.1016/j.biortech.2009.01.074

Nasser, R., Salem, M. Z. M., Hiziroglu, S., Al-Mefarrej, H., Mohareb, A., Alam, M., and Aref, I. (2016). "Chemical analysis of different parts of date palm (*Phoenix*

dactylifera L.) using ultimate, proximate and thermo-gravimetric techniques for energy production," *Energies* 9(5), Article number 374. DOI: 10.3390/en9050374

Norström, E., Fogelström, L., Nordqvist, P., Khabbaz, F., and Malmström, E. (2014). "Gum dispersions as environmentally friendly wood adhesives," *Ind. Crop. Prod*. 52, 736-744. DOI: 10.1016/j.indcrop.2013.12.001

Ramires, E. C., Megiatto, Jr., J. D., Gardrat, C., Castellan, A., and Frollini, E. (2010). "Biobased composites from glyoxal–phenolic resins and sisal fibers," *Bioresource Technol.* 101(6), 1998-2006. DOI: 10.1016/j.biortech.2009.10.005

Sahoo, S., Seydibeyoğlu, M. Ö., Mohanty, A. K., and Misra, M. (2011). "Characterization of industrial lignins for their utilization in future value added applications," *Biomass Bioenerg*. 35(10), 4230-4237. DOI: 10.1016/j.biombioe.2011.07.009

Santiago-Medina, F., Foyer, G., Pizzi, A., Caillol, S., and Delmotte, L. (2016). "Lignin-derived non-toxic aldehydes for ecofriendly tannin adhesives for wood panels," *Int. J. Adhes. Adhes*. 70, 239-248. DOI: 10.1016/j.ijadhadh.2016.07.002

Siddiqui, H. (2013). *Production of Lignin-based Phenolic Resin Using De-polymerized Kraft Lignin and Process Optimization*, Master's Thesis, The University of Western Ontario, London, Canada.

Sun, R., Tomkinson, J., and Jones, G. L. (2000). "Fractional characterization of ash-AQ lignin by successive extraction with organic solvents from oil palm EFB fibre," *Polym. Degrad. Stabil.* 68(1), 111-119. DOI: 10.1016/S0141-3910(99)00174-3

Sun, S. N., Li, M. F., Yuan, T. Q., Xu, F., and Sun, R. C. (2012). "Sequential extractions and structural characterization of lignin with ethanol and alkali from bamboo (*Neosinocalamus affinis*)," *Ind. Crop. Prod.* 37(1), 51-60. DOI: 10.1016/j.indcrop.2011.11.033

TAPPI T203 cm-09. (2009). "Alpha-, Beta- and Gamma-Cellulose in Pulp," Technical Association of the Pulp and Paper Industry, Atlanta, GA, USA.

TAPPI T222 om-02. (2006). "Acid-insoluble lignin in wood and pulp," Technical Association of the Pulp and Paper Industry, Atlanta, GA, USA.

TAPPI T650 cm-15. (2015). "Solids content of black liquor," Technical Association of the Pulp and Paper Industry, Atlanta, GA, USA.

Tejado, A., Pena, C., Labidi, J., Echeverria, J. M., and Mondragon, I. (2007). "Physico-chemical characterization of lignins from different sources for use in phenol–formaldehyde resin synthesis," *Bioresource Technol*. 98(8), 1655-1663. DOI: 10.1016/j.biortech.2006.05.042

Thring, R. W., Chornet, E., Bouchard, J., Vidal, P. F., and Overend, R. P. (1990). "Characterization of lignin residues derived from the alkaline hydrolysis of glycol lignin," *Can. J. Chem*. 68(1), 82-89. DOI: 10.1139/v90-017

Thring, R. W., Chornet, E., Bouchard, J., Vidal, P. F., and Overend, R. P. (1991). "Evidence for the heterogeneity of glycol lignin," *Ind. Eng. Chem. Res.* 30(1), 232-240. DOI: 10.1021/ie00049a036

Trick, K. A., and Saliba, T. E. (1995). "Mechanisms of the pyrolysis of phenolic resin in a carbon/phenolic composite," *Carbon* 33(11), 1509-1515. DOI: 10.1016/0008-6223(95)00092-R

Trosa, A., and Pizzi, A. (1998). "Industrial hardboard and other panels binder from waste lignocellulosic liquors/phenol-formaldehyde resins," *Holz. Roh. Werkst*. 56(4), 229-233. DOI: 10.1007/s001070050307

Váquez-Torres, H., Canché-Escamilla, G., and Cruz-Ramos, C. A. (1992). "Coconut husk lignin. I. Extraction and characterization," *J. Appl. Polym. Sci*. 45(4), 633-644. DOI: 10.1002/app.1992.070450410

Wang, S., Yu, Y., and Di, M. (2018). "Green modification of corn stalk lignin and preparation of environmentally friendly lignin-based wood adhesive," *Polymers-Basel* 10(6), Article no. 631. DOI: 10.3390/polym10060631

Wu, G. (1997). "Low-volatile and strongly basic tertiary amino alcohols as catalyst for the manufacture of improved phenolic resins," U. S. Patent No. 5623032.

Younesi-Kordkheili, H. (2019). "Ionic liquid modified lignin-phenol-glyoxal resin: A green alternative resin for production of particleboards," *J. Adhesion* 95(12), 1075-1087. DOI: 10.1080/00218464.2018.1471994

Younesi-Kordkheili, H., and Pizzi, A. (2019). "Some of physical and mechanical properties of particleboard panels bonded with phenol-lignin-glyoxal resin," *J. Adhesion* 1-11. DOI: 10.1080/00218464.2019.1600405

Zhang, W., Ma, Y., Wang, C., Li, S., Zhang, M., and Chu, F. (2013). "Preparation and properties of lignin–phenol–formaldehyde resins based on different biorefinery residues of agricultural biomass," *Ind. Crop. Prod.* 43, 326-333. DOI: 10.1016/j.indcrop.2012.07.037

Article submitted: February 19, 2021; Peer review completed: April 11, 2021; Revised version received and accepted: April 21, 2021; Published: April 26, 2021.
DOI: 10.15376/biores.16.2.4106-4125